Pol. J. Environ. Stud. Vol. 33, No. 1 (2024), 727-739
DOI: *10.15244/pjoes/171687*

Original Research

Hydro-Chemical Characteristics, Genesis Analysis and Risk Assessment of Fuyuan Laochang Ore Concentration Area in Yunnan, China

Honghao Liu[1], Yang Fan[2], Yiqi Ma[1], Chengzhong He[1], Jun Li[1], Fei Gong[1], Zhiping Zhu[1], Pingfan Zhou[3]*

[1]Kunming General Survey of Natural Resources Center, China Geological Survey, Kunming 650100, China
[2]Beijing Key Laboratory of Farmland Soil Pollution Prevention and Remediation, College of Resources and Environmental Sciences, China Agricultural University, Beijing 100193, China
[3]School of Environment, Tsinghua University, Beijing 100084, China

Received: 19 May 2023
Accepted: 30 August 2023

Abstract

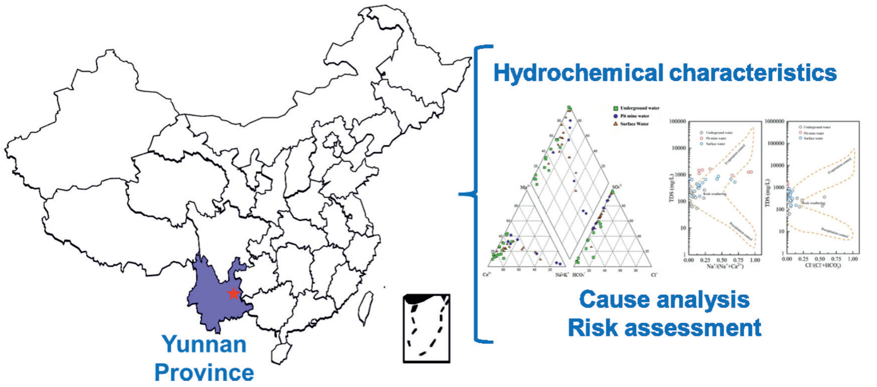

In order to reveal the characteristics of groundwater circulation in a typical basin in the mine area, the groundwater of different aquifers in Fuyuan Laochang Town, east of Qujing City, Yunnan Province, was taken as the research object. The recharge characteristics of groundwater in the study area were determined, and the material sources of the main constituents of groundwater were identified. Also, the water-rock interaction processes occurring in the study area were identified by analyzing conventional water chemistry and hydrogen and oxygen isotopes. The results show that the anions of water samples in the study area are mainly SO_4^{2-} and HCO_3^-, while the cations are mainly Na^+, Ca^{2+} and Mg^{2+}. The groundwater in the study area is mainly recharged by local atmospheric precipitation, and water vapor condensation may exist in the pit water and some underground water samples. The water-

---

*e-mail: zhoupingfan@mail.tsinghua.edu.cn

rock interaction in the study area is dominated by the lixiviation of carbonate and sulfate minerals, accompanied by silicate lixiviation and ion exchange, and the groundwater is mainly controlled by rock weathering. Domestic sewage and coal mining activities lead to the content increase of NO_3^- and SO_4^{2-} in groundwater, as well as the excess of iron and manganese ions. The corresponding results can provide a scientific basis for the protection, development, and utilization management of local groundwater resources.

Keywords: characteristics of water cycle, hydrogen and oxygen isotopes, hydro-chemical characteristics, water-rock interaction

Introduction

Mine mining activities have caused inevitable pollution and damage to surface water and groundwater [1]. Coal mining activities have led to the destruction of aquifer levels, a decline in groundwater levels, poor water quality, and a decrease in spring flow [2, 3]. Since the 1990s, with the closure of a large number of mines in Yunnan province, pit mine water may enter the adjacent soil-groundwater system, causing regional soil and groundwater pollution [4, 5]. Pit water, washing wastewater and leaching water from waste heap produced during coal mine production are the main sources of soil and water pollution, resulting in the exceedance of S, Fe, Mn and other indicators in the water bodies around the mine catchment area, and a tight supply of safe domestic water in the mine catchment area [6].

In recent years, the contradiction between the demand for water resources and the lack of resource storage has become increasingly intense. Years of underground coal mining has led to the destruction of aquifers, a general decline in the groundwater level, depletion of springs, deterioration of water quality, and an increase in the depth of mining wells year by year [7]. The irrigation of polluted water has led to increasing contamination in the soil, resulting in contaminated crops and vegetable also has seriously affected human health [8-10]. The shortage of water resources and the scientific and rational use of the problem has become an important challenge for the sustainable development of the economy. The mining concentration area of Fuyuan Laochang is one of the most prominent mining catchment areas in Yunnan, with more prominent environmental problems, among which water and soil environmental pollution caused by coal mines is the most prominent. Therefore, there is an urgent need to conduct systematic research on scientific issues such as the source and recharge mode of groundwater in the study area, in order to clarify the recharge mechanism and transport characteristics of groundwater in the typical basin of Rongjia River in Laochang, the degree of influence of surface water and groundwater transformation relationship on groundwater, and to promote the rational use of local water resources.

Stable hydrogen-oxygen isotope and water chemistry methods are effective methods for analyzing groundwater circulation, recharge sources and transformations, and are also the basis for understanding the conditions for recharge of drainage runoff in the mine and for determining the specific location of the source of sudden water in the mine [11-13], as well as for speculating the main sources of water chemistry in groundwater in the mine and the mechanism of its formation [14]. Wang et al. [15] used hydrogen-oxygen isotope methods and scanning electron microscopy of subminerals to conclude that the mineralizing fluids of the three mineralizations have different geochemical characteristics. Hao et al. [16] explored the causes of isotopic drift phenomenon and revealed the isotopic drift characteristics of karst water in Ordovician tuffs caused by coal mining. Chen et al. [17] used stable hydrogen-oxygen isotope and water chemistry to find that the mineralizing fluid of the Nuri deposit was a relatively high-temperature, highly mineralized magmatic fluid that mixed with low-temperature, low-mineralized atmospheric water during evolution. These studies have greatly improved the understanding of regional water cycle processes and laid the scientific foundation for the rational use of regional water resources. In general, many previous works have been carried out mainly from coal gangue leaching and surface groundwater pollution in mining areas, but the study of groundwater recharge-runoff-discharge relationship and groundwater chemical characteristics of different strata in the tectonic zone by analyzing typical watershed as a unit can be rare.

Based on the current limitations, we analyze the characteristics of the hydrochemical composition of surface water and groundwater and the sources of the main ions in groundwater through field sampling investigation and indoor analysis, using surface groundwater hydrogen and oxygen isotope techniques combined with water chemistry analysis methods and regional geological characteristics, to clarify the constraints on the evolution of groundwater and the spatial composition of hydrogen and oxygen isotopes, to clarify the main sources of recharge between surface water and groundwater, and to clarify the hydrological characteristics such as inter-recharge and inter-transformation relationships. It also provides a basis for rational development, protection and utilization of groundwater resources and evaluation of water quality in the mine area, and is of great significance for the study of the chemical causes and evolution of the groundwater in the old plant mine.

Materials and Methods

Sample Collection

The study area is located in Laochang Town in the southeastern part of Fuyuan County, adjacent to Huangnihe Town in the east, with the geographical location ranging from 104°30′ to 104°35′E and 25°11′ to 25°16′N (Fig. 1). The area of Laochang Town is about 236 km^2, and the terrain is mainly mountainous, with elevation of 1480~2460 m, of which the karst area is about 159 km^2, located in the subtropical plateau monsoon climate area, with obvious three-dimensional climate, annual average temperature of 11-14ºC, rainfall mostly concentrated in May-October, annual rainfall of 1100-1500 mm, and average evaporation of 1885.5 mm. The regional geological work area is located in the old plant tectonic zone, which is oriented at 40°-45°N.E., with a length of about 20 km and a width of about 6 km.

The tectonic zone is mainly composed of the Old Plant backslope, the foot fractures parallel to the backslope and the Sulphur Plant fracture, which are all compression-torsional in nature. The exposed strata in the study area consist of the Lower Permian Mao Kou Formation tuffs, Upper Permian Longtan Formation tuffs, mudstones, siltstones, sandstones and coal beds, and the Lower Triassic Feixianguan Formation chip sandstones, rock chip siltstones and muddy siltstones. Groundwater mainly includes pore water of the loose layer of the Fourth Series, fracture water of coal clastic rock and fracture water of carbonate karst, etc. In this experiment, water samples of river water, groundwater, mine pit water and coal gangue drainage water were collected from the mine catchment area of Rongjia River Basin in Laochang in September 2020 (abundant water period) and March 2021 (dry water period), respectively. A total of 14 groups of isotope water samples were collected, including 12 groups of groundwater samples, 2 groups of river water samples; 14 groups of groundwater full analysis samples, 7 groups of mine water analysis samples and 16 groups of surface water samples (Fig. 2). The groundwater was divided into groundwater from the clastic rocks of the Triassic Feixianguan group, groundwater from the coal bed of the Permian Longtan group and groundwater from the chert of the Permian Maokou group, and the groundwater samples collected in this paper were mainly springs and deep groundwater from boreholes.

Testing Method

Sampling apparatus in accordance with the prescribed standards using polyethylene plastic bottles and brown hard glass bottles, sample bottles cleaned in advance with distilled water, and then rinsed with water samples 3 times before sampling [18]. The sampling bottle into the water filled with no air bubbles, the scene to add a good protective agent after sealing, low temperature storage and avoid direct sunlight. Groundwater sampling before letting it flow for 3-5 minutes, borehole sampling before pumping 10-15 minutes, surface water sampling sample bottle to the central river below the liquid level sampling. On-site use of portable multi-parameter water quality meter (DZB-718, Leici Co., Ltd, China) to determine the pH, temperature (T), electrical conductivity (EC)

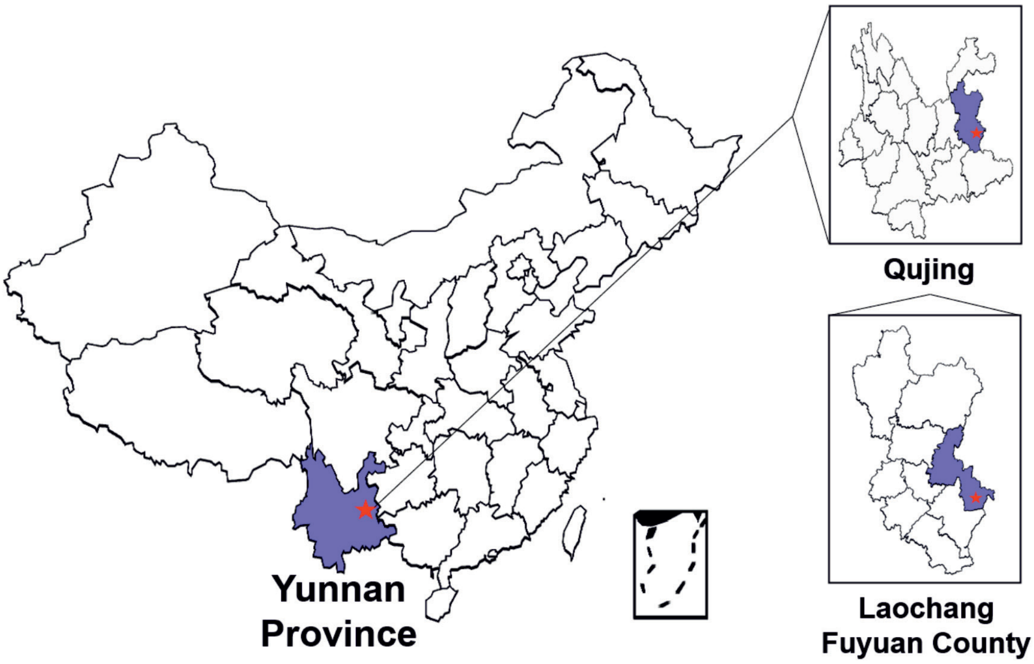

Fig. 1. Locations of in Laochang in the map of China.

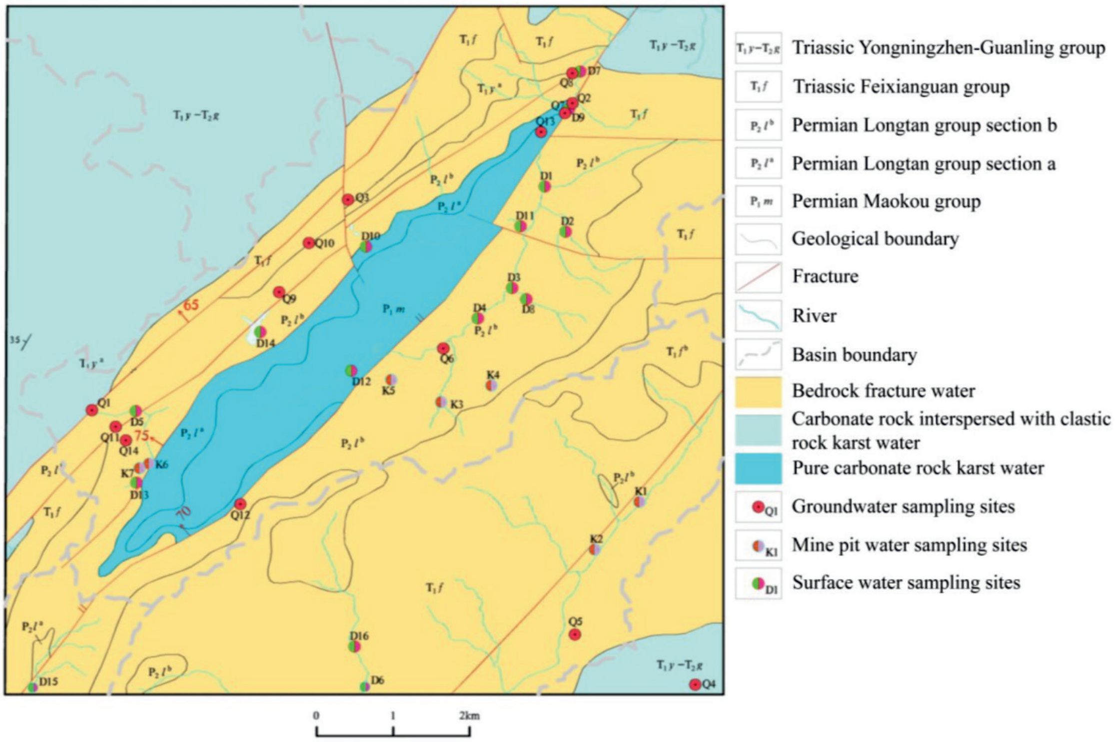

Fig. 2. Locations of sampling sites in Laochang.

and mineralization (TDS) and other physicochemical parameters of water samples at the sampling site. The physical and chemical parameters such as K^+, Na^+, Ca^{2+}, Mg^{2+} and metal content in the water are determined according to the relevant national standards of China [19-21]. Hydrogen (δD) and oxygen (δ18O) isotopes were determined using stable gas isotope mass spectrometer (253Plus, ThermoFisher Scientific, USA). All samples are additionally tested for two parallel samples to control the quality of analysis and testing. The isotopes were tested by testing the standard samples at the same time to ensure the quality, which ensured the real credibility of the analysis results.

Results and Discussion

Type of Water Chemistry

The results of water chemistry element testing at the water sample sites in the study area are shown in Table 1. Water chemistry type analysis was performed using Aquachem software to obtain the piper trilinear diagram (Fig. 3) [22]. The anions in the groundwater samples of the study area were dominated by HCO^{3-} and $SO4^{2-}$, and the cations were dominated by Ca^{2+} and Mg^{2+}. The water chemistry types can be divided into HCO_3-Ca, SO_4·HCO_3-Ca·Mg, SO_4·HCO_3-Ca, HCO_3·SO_4-Ca, and HCO_3·SO_4-Ca·Mg, among which the HCO_3-Ca type was dominant. The anions in the pit mine water samples are mainly SO_4^{2-} and HCO_3^-, and the cations are mainly Na^+, Ca^{2+} and Mg^{2+}. The water chemistry types can be divided into SO_4-HCO_3-Na, SO_4-HCO_3-Ca-Mg, SO_4-Ca-Mg, etc., among which SO_4-HCO_3-Na and SO_4-Ca-Mg are mainly. The anions in surface water samples are mainly SO_4^{2-} and HCO_3^-, and the cations are mainly Na^+, Ca^{2+} and Mg^{2+}, and the water chemistry types can be divided into SO_4·HCO_3-Ca·Mg, SO_4·HCO_3-Ca, SO_4-Ca·Mg, SO_4-Ca, SO_4·HCO_3-Na·Ca, HCO_3·SO_4-Ca, HCO_3·SO_4-Na·Ca, etc., with SO_4·HCO_3-Ca·Mg, SO_4·HCO_3-Ca, and SO_4-Ca·Mg dominating (Fig. 3).

The study area is located in Yunnan, which is a typical karst landscape area [23], where the dissolution and precipitation of soluble rocks by groundwater and surface water are more obvious [24]. The reaction between the infiltrated recharged atmospheric precipitation and the overlying carbonate and saltstone minerals of the Maokou Formation and the pyrite and chalcopyrite minerals within the coal seam of the Longtan Formation, resulting in the generally high contents of HCO_3^-, SO_4^{2-}, Ca^{2+} and Mg^{2+} in the water samples of the study area [25, 26]. Similarly higher HCO_3^-, SO_4^{2-}, Ca^{2+} and Mg^{2+} were also observed in other study areas in Yunnan [25, 27, 28].

Recharge Characteristics of Groundwater

As can be seen from Table 1, the main ions of water samples in the study area are Ca^{2+}, Mg^{2+}, Na^+, HCO_3^-, and SO_4^{2-}, and their sources are closely related to the lithology of the aquifer [29]. The area is mainly carbonate rocks as well as clastic rocks, and the dissolution filtration or precipitation of carbonate as well as silicate minerals affects the ionic composition in the groundwater of the study area [28, 30]. The analysis of the ion scale factor (Fig. 4) can effectively determine the main water-rock action in the study area [31]. Fig. 4a) shows the ratio of Ca^{2+} to SO_4^{2-}. The value of Ca^{2+}/SO_4^{2-} in groundwater is basically greater than 1:1, and there may be dissolution of carbonate minerals such as calcite ($CaCO_3$) and dolomite ($CaMg(CO_3)_2$)), and the dissolution equation is shown in Equation (1) and Equation (2). The Ca^{2+}/SO_4^{2-} value of surface water is basically close to 1:1, which shows that Ca^{2+} and SO_4^{2-} in water basically originate from the dissolution of gypsum ($CaSO_4{\cdot}2H_2O$), and the dissolution equation is shown in Equation (3). The ratio of pit mine water and some surface water samples is less than 1:1, and the SO_4^{2-} content is too much, so there may be a cation exchange process (Equation (4)), which makes some Ca^{2+} replaced by Na^+ [32].

$$CaCO_3 + CO_2(g) + H_2O \leftrightarrow Ca^{2+} + 2HCO_3^- \tag{1}$$

$$CaMg(CO_3)_2 + 2CO_2(g) + 2H_2O \leftrightarrow Ca^{2+} + Mg^{2+} + 4HCO_3^- \tag{2}$$

$$CaSO_4 \cdot 2H_2O \leftrightarrow Ca^{2+} + SO_4^{2-} + 2H_2O \tag{3}$$

$$2NaX + Ca^{2+} \leftrightarrow 2Na^+ + CaX_2 \tag{4}$$

Fig. 4b) shows the ratio of Na^+ to Cl^-. The points of Na^+/Cl^- values in groundwater, pit mine water and surface water are all located above the rock salt dissolution line with a ratio of 1:1, indicating that feldspar weathering and silicate mineral reactions may have occurred, or cation exchange, where Ca^{2+} is adsorbed onto clay minerals, allowing Na^+ ions to be replaced and their content to increase [33]. As shown in Fig. 4c), the values of $(Ca^{2+}+Mg^{2+})/(HCO_3^-+SO_4^{2-})$ in groundwater and most of surface water are on the 1:1 line, indicating that Ca^{2+}, Mg^{2+}, HCO_3^-, and SO_4^{2-} in water originate from the dissolution of carbonate minerals and sulfate minerals mainly, which verifies each other with the conclusion in Fig. 3a) [34]. Fig. 4d) shows the values of $[(Ca^{2+}+Mg^{2+}) - (HCO_3^-+SO_4^{2-})]/(Na^+ - Cl^-)$, and all points are very close to the ideal value of -1, indicating that silicate dissolution and ion exchange interactions jointly influence the type of hydro-chemical interactions in the study area [35].

The ion exchange can be analyzed by Chloro-Alkaline Indices (CAI) [36], as shown in Equation (5). If the CAI is negative, it means that Ca^{2+} and Mg^{2+} in groundwater exchange ions with Na^+ in the aqueous medium; if its value is positive, the Na+ in groundwater is replaced by Ca^{2+} and Mg^{2+}. As shown in Table 1, the CAI -I values of the water samples are all negative, indicating that the replacement of Ca^{2+} and Mg^{2+} in water by Na^+ in the water-bearing medium minerals is the main ion exchange process in the study area [37].

$$CAI - I = \frac{Cl^- - (Na^+ + K^+)}{Cl^-} \tag{5}$$

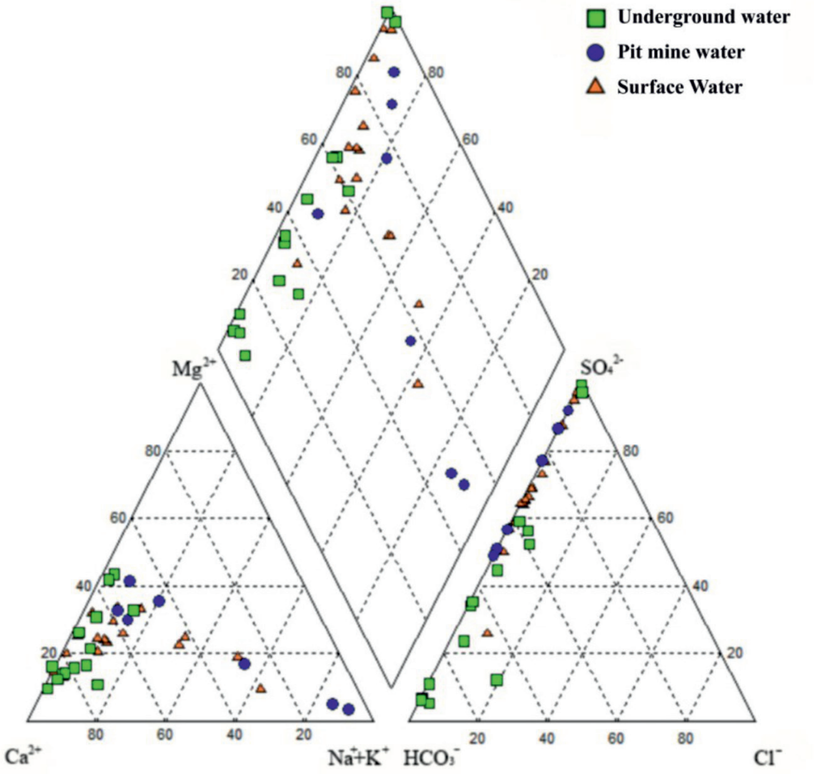

Fig. 3. Piper diagram of water chemistry of water samples in the study area.

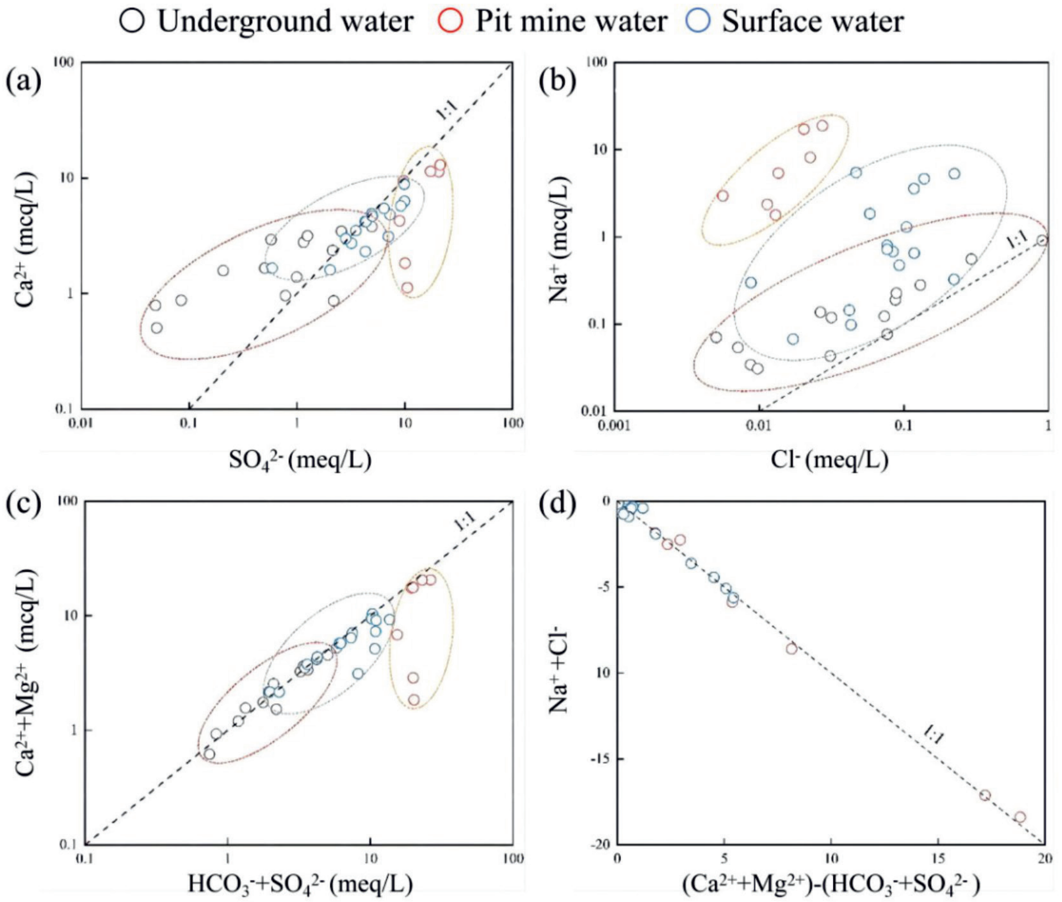

Fig. 4. Proportion of major ions in water samples in the study area.

Sources of Main Groundwater Components

Hydrogen-oxygen isotope and water chemistry methods of water bodies are effective ways to study the water cycle, and stable hydrogen-oxygen isotope composition is an effective tracer to reveal the physicochemical processes of the water cycle, which plays an important role in studying the source and mode of groundwater recharge in the basin and the mutual transformation process of surface water and groundwater [14, 38-41]. A total of 14 sets of water samples were collected for hydrogen and oxygen isotope testing (Table 2), including 10 sets of groundwater samples, 2 sets of pit mine water samples, and 2 sets of surface water samples. The δD values of groundwater and pit mine water in the study area varied from -82.9 to -75.3 with a mean value of -78.82, and the δ18O values varied from -14.16 to -11.01 with a mean value of -12.13.

Craig (1961) proposed that the hydrogen-oxygen isotopic composition of atmospheric precipitation is linearly correlated [42]: $\delta D = 8\delta^{18}O + 10$, which is the accepted global meteoric water line (GMWL) [43]. The atmospheric precipitation line in the study area was selected from the east Yunnan-Qianxi atmospheric precipitation line with the relationship: $\delta D = 7.848\delta^{18}O + 11$. As shown in Fig. 5, the surface water sample points in the study area were distributed on the local atmospheric precipitation line, and most of the groundwater and surface water samples were distributed near the local atmospheric precipitation line, indicating that the groundwater mainly originated from atmospheric precipitation; however, the pit mine water and three groundwater samples, TW02, TW03 and TW05, were shifted, and the $\delta^{18}O$ values decreased and were located to the left of the atmospheric precipitation line. According to Pang et al. (2016) the relationship between hydrogen and oxygen isotopes is divided into 13 lines [44], the points in the study area that are offset from the local atmospheric precipitation line are close to line 10 (Eq. (6)). For example, there is condensation of water vapor, resulting in low values of both hydrogen and oxygen isotopes with small slopes [45].

$$\delta^2 H = n\delta^{18}O + d\ (n < 8, \delta^{18}O < \delta^{18}O_{GWML}) \quad (6)$$

Gibbs plot can be effectively analyzed by $Na^+/(Na^+ + Ca^{2+})$ and $Cl^-/(Cl^- + HCO_3^-)$ compared with TDS, respectively (Fig. 7). The types of water chemistry can be classified into: "evaporation-controlled", "rock-weathering" and "precipitation-controlled" [46]. Fig. 7 shows the Gibbs plot of the sampling points in the study area. The TDS ranges of groundwater and surface water

Table 1. Results of water chemistry in the study area.

Number	Type of water sample	pH	Concentration (mg/L)											Type of water chemistry	CAI-I
			K^+	Na^+	Ca^{2+}	Mg^{2+}	Cl^-	SO_4^{2-}	HCO_3^-	NO_3^-	Fe	Mn	TDS		
Q1	Groundwater	8.17	12.10	20.90	58.80	5.26	32.10	27.60	196.00	1.77	<0.01	0.01	268	HCO_3-Ca	-0.35
Q2	Groundwater	7.90	0.70	3.15	55.60	5.65	0.94	55.30	133.00	0.78	<0.01	0.07	204	$HCO_3\cdot SO_4$-Ca	-4.85
Q3	Groundwater	8.86	0.45	0.79	17.50	3.89	0.31	4.05	70.40	2.54	<0.01	<0.01	72	HCO_3-Ca·Mg	-4.27
Q4	Groundwater	7.69	0.21	0.99	15.80	1.66	1.10	2.34	50.00	0.50	<0.01	<0.01	64	HCO_3-Ca	-0.56
Q5	Groundwater	7.35	0.40	1.62	10.10	1.36	0.18	2.40	44.50	1.77	0.07	<0.01	56	HCO_3-Ca	-15.00
Q6	Groundwater	7.72	11.80	12.80	69.10	8.52	10.40	124.00	104.00	7.79	<0.01	0.54	330	$SO_4\cdot HCO_3$-Ca	-1.93
Q7	Groundwater	7.95	0.67	2.74	63.20	5.61	1.12	60.10	137.00	1.29	<0.01	0.03	216	$HCO_3\cdot SO_4$-Ca	-3.32
Q8	Groundwater	7.02	1.17	2.83	27.80	13.90	2.60	47.70	70.40	5.01	<0.01	<0.01	160	$HCO_3\cdot SO_4$-Ca·Mg	-1.09
Q9	Groundwater	4.01	0.42	1.24	17.30	7.97	0.25	105.00	0.39	0.19	<0.01	0.70	148	SO_4-Ca·Mg	-8.08
Q10	Groundwater	8.17	0.35	0.71	31.60	2.07	0.35	9.94	100.00	0.31	<0.01	<0.01	105	HCO_3-Ca	-3.10
Q11	Groundwater	7.21	0.38	4.36	33.20	6.13	3.10	24.10	92.70	4.35	<0.01	0.02	140	HCO_3-Ca	-1.28
Q12	Groundwater	5.15	4.23	1.76	76.10	8.84	2.72	238.00	3.70	3.82	<0.01	1.04	370	SO_4-Ca	-1.41
Q13	Groundwater	8.25	2.01	5.21	47.30	13.70	3.15	103.00	85.20	2.64	0.96	0.09	242	$SO_4\cdot HCO_3$-Ca·Mg	-2.13
Q14	Groundwater	7.52	0.74	6.48	19.20	7.27	4.62	37.50	35.20	6.49	0.03	<0.01	134	$SO_4\cdot HCO_3$-Ca·Mg	-1.31
K1	Pit mine water	7.00	1.96	434.00	22.50	8.65	0.97	507.00	619.00	0.80	2.29	0.25	1292	$SO_4\cdot HCO_3$-Na	-691.43
K2	Pit mine water	7.60	2.30	396.00	36.70	12.40	0.72	482.00	636.00	1.34	1.02	0.09	1260	$SO_4\cdot HCO_3$-Na	-846.11
K3	Pit mine water	9.65	2.35	188.00	85.40	30.90	0.80	430.00	415.00	2.01	18.47	0.35	962	$SO_4\cdot HCO_3$-Na	-364.39
K4	Pit mine water	7.89	3.03	41.00	190.00	96.40	0.46	467.00	617.00	1.72	0.76	0.12	1124	$SO_4\cdot HCO_3$-Ca·Mg	-142.57
K5	Pit mine water	8.20	4.64	124.00	227.00	111.00	0.48	990.00	374.00	3.15	16.33	0.86	1656	SO_4-Ca·Mg	-405.68
K6	Pit mine water	6.99	3.90	54.30	260.00	90.60	0.40	1022.00	11300	0.11	61.60	1.99	1484	SO_4-Ca·Mg	-215.78
K7	Pit mine water	6.53	3.74	67.87	228.17	74.81	0.20	832.00	163.94	0.05	91.97	2.04	1518	SO_4-Ca·Mg	-542.51
D1	Surface Water	8.15	3.26	15.60	70.20	20.80	2.98	169.00	145.00	2.41	1.13	0.19	374	$SO_4\cdot HCO_3$-Ca·Mg	-8.08
D2	Surface Water	7.66	1.41	10.90	54.60	19.70	3.30	154.00	66.70	5.29	3.30	0.40	312	SO_4-Ca·Mg	-4.49
D3	Surface Water	7.31	3.03	82.30	96.30	29.50	4.17	350.00	230.00	2.20	3.89	0.71	694	$SO_4\cdot HCO_3$-Ca·Na	-30.12
D4	Surface Water	8.16	2.79	29.90	98.10	26.10	3.70	237.00	163.00	3.07	1.61	0.34	504	$SO_4\cdot HCO_3$-Ca·Mg	-12.16
D5	Surface Water	7.59	2.97	7.48	33.20	6.02	7.88	28.20	88.90	4.27	0.17	0.03	158	$HCO_3\cdot SO_4$-Ca	-0.81

Table 1. Continued.

D6	Surface Water	8.67	1.97	122.00	46.30	9.69	7.93	207.00	249.00	1.92	3.94	0.17	534	$HCO_3 \cdot SO_4$-$Na \cdot Ca$	-22.97
D7	Surface Water	8.03	2.34	18.40	84.20	18.30	2.72	206.00	113.00	2.43	4.26	0.54	409	$SO_4 \cdot HCO_3$-Ca	-10.22
D8	Surface Water	7.55	1.90	126.00	62.50	24.30	1.66	339.00	237.00	2.01	5.65	0.30	692	$SO_4 \cdot HCO_3$-$Na \cdot Ca$	-117.20
D9	Surface Water	8.86	2.30	16.60	84.10	18.80	2.72	210.00	117.00	2.39	5.30	0.61	412	$SO_4 \cdot HCO_3$-Ca	-9.19
D10	Surface Water	7.55	2.96	3.32	177.00	18.60	1.49	474.00	29.60	0.26	19.90	1.55	712	SO_4-Ca	-4.25
D11	Surface Water	7.70	1.52	2.26	59.90	9.26	1.53	136.00	50.00	2.00	6.47	0.70	252	SO_4-Ca	-2.18
D12	Surface Water	7.17	3.36	15.00	93.70	20.70	4.18	240.00	148.00	2.25	1.14	0.84	460	$SO_4 \cdot HCO_3$-Ca	-5.27
D13	Surface Water	5.30	0.92	6.88	126.00	37.80	0.31	477.00	16.70	0.08	0.26	3.66	668	SO_4-$Ca \cdot Mg$	-35.84
D14	Surface Water	5.94	0.71	1.55	32.00	6.75	0.61	97.70	16.70	0.13	0.37	0.67	158	SO_4-$Ca \cdot Mg$	-3.99
D15	Surface Water	7.85	2.98	42.5	109.00	43.80	2.07	308.00	293.00	0.88	0.50	0.66	666	$SO_4 \cdot HCO_3$-$Ca \cdot Mg$	-32.00
D16	Surface Water	8.32	3.06	107.00	115.00	41.80	4.91	442.00	285.00	2.47	6.26	0.25	876	$SO_4 \cdot HCO_3$-$Ca \cdot Mg$	-33.20

are 56~370 mg/L and 158~876 mg/L, respectively, which are freshwater; the pit mine water has the highest TDS, ranging from 962~1656 mg/L, which are brackish water except for point KKS11. All water sample points fall in the rock weathering control area, which shows that the groundwater in the study area is mainly controlled by rock weathering [47].

Water-Rock Action Analysis

The saturation index (SI) is a parameter to study the saturation state of minerals in groundwater, which has an important indication in the study of water-rock interaction and is defined as [48]:

$$SI = lg\frac{LAP}{K} \tag{7}$$

In Equation (7), LAP is the activity product of the relevant ions in the dissolution reaction of minerals; K is the equilibrium constant of the dissolution reaction of minerals at a specific temperature. When SI<0, it indicates that the mineral is in an unsaturated state in solution; when SI = 0, the mineral is in dissolution equilibrium in solution; when SI>0, the mineral is supersaturated in solution.

According to the water chemistry results, the main cations at the water sample sites are Na^+, Ca^{2+}, and Mg^{2+}, and the main anions are SO_4^{2-} and HCO_3^-. Therefore, the possible mineral phases in the study area are calcite, dolomite, gypsum, and anhydrous gypsum. The saturation index of each mineral was calculated using PHREEQC geochemical software [49], and the results are shown in Fig. 8. The SI values of calcite at each water sample point are close to 0, that is, calcite is basically in dissolution equilibrium, and there may be mineral precipitation if it continues to dissolve [50]; the SI values of the remaining minerals (dolomite, gypsum, anhydrous gypsum) are basically less than 0, which are in unsaturated state, indicating that the water samples in the study area have the ability to continue to dissolve the surrounding rocks [48]. Furthermore, the ratio of pit mine water to some surface water is on the 1 :1 line (Fig. 3c), suggesting that other water-rock interactions are involved [51].

Water Risk Assessment in Mining Areas

It is worth noting that the study area contains relatively extensive semi-metallic deposits, so the risk of elemental exceedances in this area requires special attention [52, 53]. We can see from the data in Table 1 that groundwater is a little more polluted than surface water. Compared with surface water pollution, groundwater contamination is much more challenging to address once it has occurred. The most direct route of contamination of aquifers in the present study area is through open pit mining or underground mining below the water table [54]. According to the groundwater

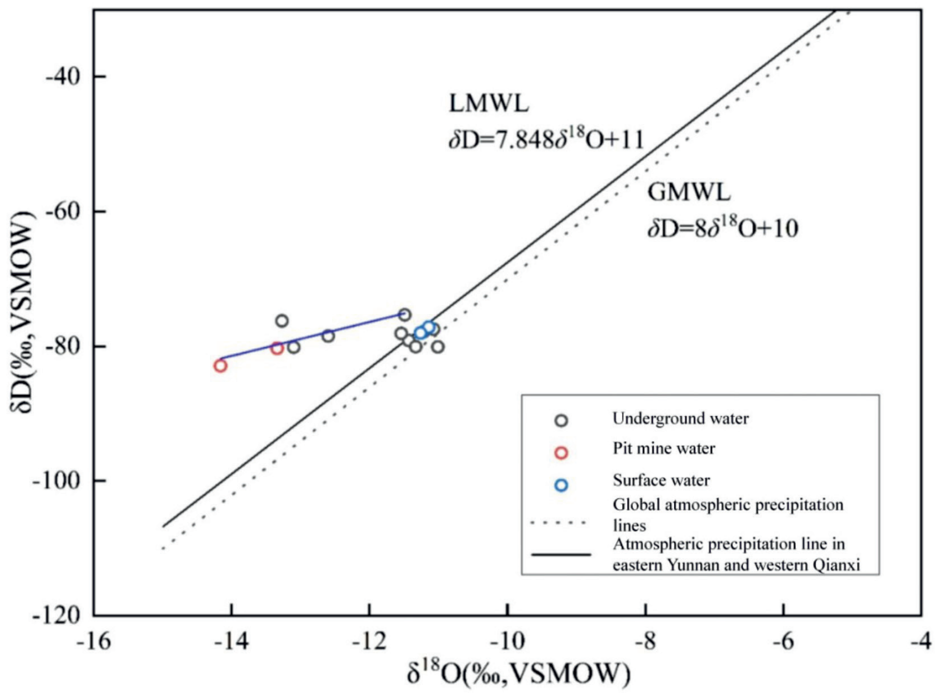

Fig. 5. Stable isotope distribution of groundwater, pit mine water and surface water.

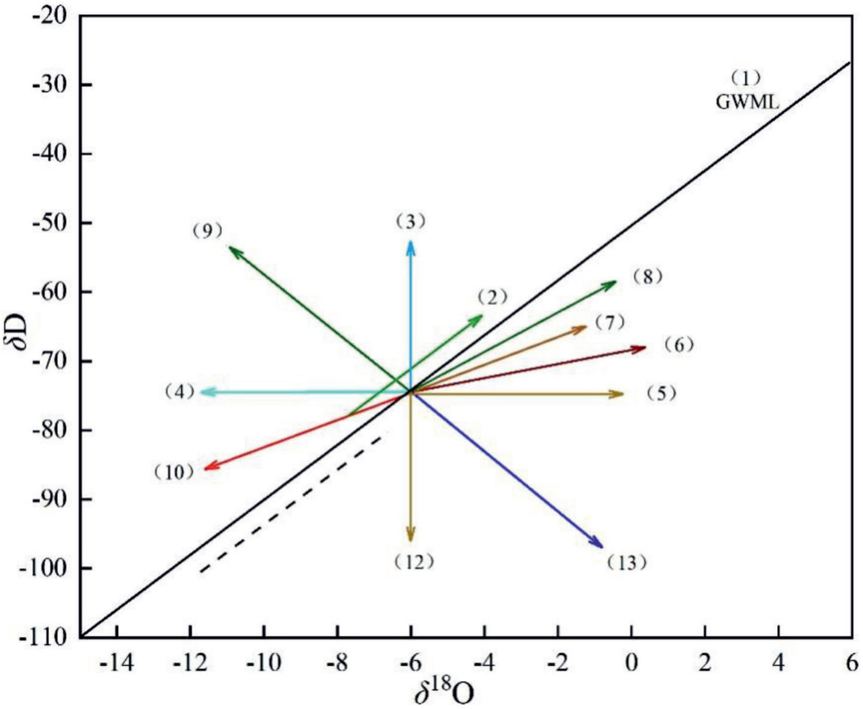

Fig. 6. Isotope geological indicators and water-rock interaction processes: (1) Global atmospheric precipitation line GMWL (2) Moisture cycle (3) H_2S exchange (4) CO_2 exchange (5) Water-rock action in underground hot water (6) Water mixing in andesite medium (7) Evaporation operation (8) Seawater mixing (9) Silicate hydrolysis (10) Water vapor condensation (11) Paleo-atmospheric water (12) Hydrocarbon exchange (13) Clay mineral exchange.

quality standards in the geological and mining industry standards of the People's Republic of China (DZ/T 0290-2015). The pH values of groundwater sampling sites Q3, Q9 and Q12 reached Class IV and V category, respectively. In terms of SO_4^- content, Q2, Q6, Q7, Q9 and Q13 sampling points are category II, and Q12 is category III. Fe content of Q13 reached IV category; Q6, Q8, and Q12 have Mn levels up to Category IV. Class IV

Table 2. Hydrogen and oxygen isotope test results of water samples in the study area.

Samples	Types	$\delta^{18}O$ (VSMOW, ‰)	δD (VSMOW, ‰)
Q1	Ground water	-11.49	-75.3
Q2	Ground water	-11.43	-79.1
Q4	Ground water	-11.54	-78.1
Q5	Ground water	-11.33	-80.0
Q7	Ground water	-11.01	-80.1
Q8	Ground water	-11.21	-77.8
Q10	Ground water	-11.07	-77.4
Q11	Ground water	-12.60	-78.5
Q12	Ground water	-13.27	-76.2
Q14	Ground water	-13.10	-80.1
K4	Pit mine water	-14.16	-82.9
K7	Pit mine water	-13.34	-80.3
D5	Surface water	-11.14	-77.1
D7	Surface water	-11.26	-78.0

and V waters are not suitable for direct use as drinking water because of their high chemical content. Excessive levels of iron and manganese not only affect the color, odor and taste of drinking water, but also have a negative impact on human health [55]. For example, excessive iron intake may cause bacterial infections, acute iron toxicity, hemochromatosis and other diseases in patients [56]; excessive manganese may cause negative reactions in the gastrointestinal tract, lesions in the oral mucosa, and neurological damage [57]. Therefore, groundwater from the above exceedance sites requires some treatment before drinking, and future research should emphasize the migration and transformation of contaminants in groundwater.

Conclusions

In this study, water chemical characteristics, source and evolution, water-rock interaction and risk assessment of water in Laochang study area were comprehensively explored through field investigation observations and sampling tests. It was found that the anions in the water samples in the study area were mainly SO_4^{2-}

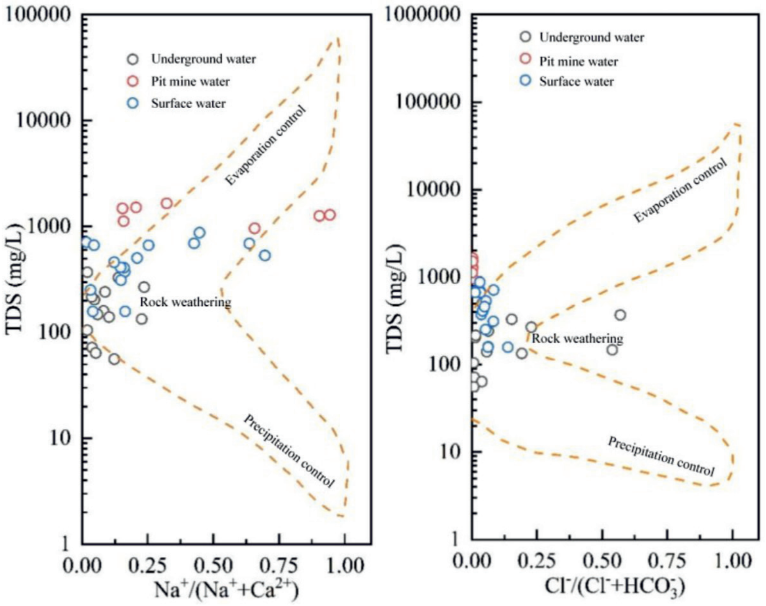

Fig. 7. Gibbs plot of sampling sites in the study area.

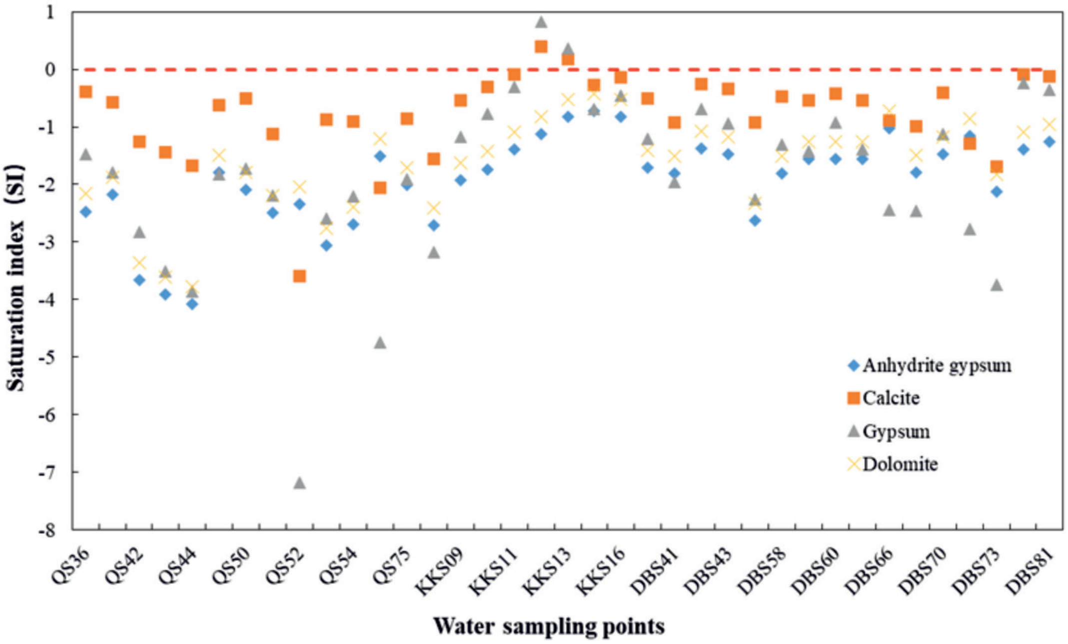

Fig. 8. Map of possible mineral phase saturation index at water sample points.

and HCO^{3-}, and the cations were mainly Na^+, Ca^{2+} and Mg^{2+}, and their water chemical element contents were closely related to the lithology of the aquifer. The results of hydrogen-oxygen isotope correlation analysis show that the groundwater in this area mainly comes from atmospheric precipitation, in which the pit mine water and some groundwater samples are offset, and there may be the phenomenon of water vapor condensation. In addition, the Gibbs diagram shows that the groundwater in the study area is mainly controlled by rock weathering. Finally, we also conducted a risk assessment of the Laochang study area, which identified some contamination exceedance points. The results of this study shed light on the water chemistry, water sources and evolution, and water-rock interactions in the Old Field, and the results of the risk assessment can also be an effective guide to improving the quality and safety of drinking water in the area.

Acknowledgments

This work was supported by Investigation of lakes in the lake area of the Yunnan-Guizhou Plateau (DD20230512), Survey on Ecological Restoration Support in Fuyuan, Yunnan Province-Panzhou, Guizhou Province Energy and Mineral Concentration Area (No. DD20208075). This work was also supported by the Ministry of Natural Resources, Carbon Sinks Engineering and Technology Innovation Center, Ministry of Natural Resources, under the project "Research on the spatial distribution characteristics, influencing factors and sources of dissolved carbon in lakes in the Yunnan-Guizhou Plateau lake area based on δ13C" ([2023]10-2302-03).

References

1. CHAMIER J., WICHT M., CYSTER L., NDINDI N.P. Aluminium (Al) fractionation and speciation; getting closer to describing the factors influencing Al^{3+} in water impacted by acid mine drainage. Chemosphere, **130**, 17, **2015**.
2. KARAN S.K., SAMADDER S.R., SINGH V. Groundwater vulnerability assessment in degraded coal mining areas using the AHP-Modified DRASTIC model. Land Degradation & Development, **29** (8), 2351, **2018**.
3. DONG S.G., FENG H.B., XIA M.H., LI Y., WANG C., WANG L. Spatial-temporal evolutions of groundwater environment in prairie opencast coal mine area: a case study of Yimin Coal Mine, China. Environmental Geochemistry and Health, **42** (10), 3101, **2020**.
4. CHEN D., FENG Q.Y., LIANG H.Q., GAO B., ALAM E. Distribution characteristics and ecological risk assessment of polycyclic aromatic hydrocarbons (PAHs) in underground coal mining environment of Xuzhou. Human and Ecological Risk Assessment, **25** (6), 1564, **2019**.
5. YANG L.Z., XU J.J., FANG J., CAO Z.G., LI T.X., SONG H.Q. Risk evaluation of groundwater leakage in coal seam goaf: a case study in the Lingxin Mining Area. Environmental Science and Pollution Research, **27** (21), 26066, **2020**.
6. GAUTHIER-MANUEL H., RADOLA D., CHOULET F., BUATIER M., VAUTHIER R., MORVAN T., CHAVANNE W., GIMBERT F. A Multidisciplinary Approach for the Assessment of Origin, Fate and Ecotoxicity of Metal(loid) s from Legacy Coal Mine Tailings. Toxics, **9** (7), 18, **2021**.
7. EL HARAOUI N., TAO T., XIN K., WANG Q. Analysis of heavy metals and ions in tap water: A case of Shanghai P District. Fresenius Environ. Bull, **23**, 395, **2014**.
8. WANG K., LIU J., MI T., ZHOU P., MUHAMMAD A., RUI Y. Comparison of copper and zinc contents in peel and pulp of apple and grape in different regions. Fresenius Environmental Bulletin, **30** (11A), 12691, **2021**.

9. ZHOU P., ADEEL M., SHAKOOR N., GUO M., HAO Y., AZEEM I., LI M., LIU M., RUI Y. Application of Nanoparticles Alleviates Heavy Metals Stress and Promotes Plant Growth: An Overview. Nanomaterials, **11** (1), 26, **2021**.
10. ZHOU P., LONG B., WANG R., JIANG Y., ZHAO W., LI Y., LI M., GUO Z., ZHANG P., RUI Y. Increase in the active ingredients of traditional Chinese medicine Isatis indigotica through iron nanoparticles supplementation versus carbon nanotubes: a comparative study. Environmental Science-Nano, **2022**.
11. RUPPEL T.C., GREIN C.T., BIENSTOCK D. Adsorption of methane on dry coal at elevated pressure. Fuel, **53** (3), 152, **1974**.
12. QIU H.L., GUI H.R., CUI L., PAN Z.G. Hydrogeochemical Processes and Quality Assessment of Groundwater in Sulin Mining Area, Northern Anhui Province, China. Water Resources, **48** (6), 991, **2021**.
13. GUO Y., GUI H.R., WEI J.C., ZHANG Z., HU M.C., FANG P., LI G.P., GAO C., WANG X. Hydrogeochemistry of Water in Coal Measures during Grouting Treatment of Taoyuan Mine, China. Groundwater, **59** (2), 256, **2021**.
14. ARUMUGAM K., ELANGOVAN K. Hydrochemical characteristics and groundwater quality assessment in Tirupur Region, Coimbatore District, Tamil Nadu, India. Environmental Geology, **58** (7), 1509, **2009**.
15. WANG K.Y., QING M., ZHANG X.N., WAN D., XIAO L. Study on the characteristics of fluid inclusions and metallogenic evolution of Jinchang gold deposit, Heilongjiang Province. Acta Petrologica Sinica, **27** (5), 1275, **2011**.
16. HAO C.M., HUANG Y., HE P.Y., SUN W. Isotope Drift Characteristics in Ordovician Limestone Karst Water Caused by Coal Mining in Northern China. Mine Water and the Environment, **38** (3), 507, **2019**.
17. CHEN L., QIN K.Z., LI J.X., XIAO B., LI G.M., ZHAO J.X., FAN X. Fluid Inclusions and Hydrogen, Oxygen, Sulfur Isotopes of Nuri Cu-W-Mo Deposit in the Southern Gangdese, Tibet. Resource Geology, **62** (1), 42, **2012**.
18. LI S., ZHANG Q. Geochemistry of the upper Han River basin, China, 1: spatial distribution of major ion compositions and their controlling factors. Applied geochemistry, **23** (12), 3535, **2008**.
19. ZHANG B., SONG X., ZHANG Y., HAN D., TANG C., YU Y., MA Y. Hydrochemical characteristics and water quality assessment of surface water and groundwater in Songnen plain, Northeast China. Water Research, **46** (8), 2737, **2012**.
20. ZHOU P., ADEEL M., GUO M., GE L., SHAKOOR N., LI M., LI Y., WANG G., RUI Y. Characterisation of biochar produced from two types of chestnut shells for use in remediation of cadmium- and lead-contaminated soil. Crop and pasture science, **2022**.
21. ZHOU P., GUO M., LI M., HAO Y., LIU M., RUI Y. Investigation and analysis of trace elements in rarmland soil in Shanghe County Shandong Province. Fresenius Environmental Bulletin, **30** (6), 5789, **2021**.
22. SELVAKUMAR S., CHANDRASEKAR N., KUMAR G. Hydrogeochemical characteristics and groundwater contamination in the rapid urban development areas of Coimbatore, India. Water Resources and Industry, **17**, 26, **2017**.
23. ZHANG X., YUE Y., TONG X., WANG K., QI X., DENG C., BRANDT M. Eco-engineering controls vegetation trends in southwest China karst. Science of The Total Environment, **770**, 145160, **2021**.
24. JI H., WANG S., OUYANG Z., ZHANG S., SUN C., LIU X., ZHOU D. Geochemistry of red residua underlying dolomites in karst terrains of Yunnan-Guizhou Plateau: I. The formation of the Pingba profile. Chemical Geology, **203** (1-2), 1, **2004**.
25. BECKFORD H.O., CHU H., SONG C., CHANG C., JI H. Geochemical characteristics and behaviour of elements during weathering and pedogenesis over karst area in Yunnan–Guizhou Plateau, southwestern China. Environmental Earth Sciences, **80**, 1, **2021**.
26. PETERS S.G., JIAZHAN H., ZHIPING L., CHENGGUI J. Sedimentary rock-hosted Au deposits of the Dian–Qian–Gui area, Guizhou, and Yunnan Provinces, and Guangxi District, China. Ore Geology Reviews, **31** (1-4), 170, **2007**.
27. ZHONG J., LI S.-L., TAO F., YUE F., LIU C.-Q. Sensitivity of chemical weathering and dissolved carbon dynamics to hydrological conditions in a typical karst river. Scientific Reports, **7** (1), 42944, **2017**.
28. SUN W., SONG J., YANG W., ZHENG Y., LI C., KUANG D. Distribution of carbonate rocks and variation analysis of karst water resources in China. Carbonates and Evaporites, **35**, 1, **2020**.
29. ASHJARI J., RAEISI E. Lithological control on water chemistry in karst aquifers of the Zagros Range, Iran. Cave and Karst Science, **33** (3), 111, **2006**.
30. LIU W.-J., LIU C.-Q., ZHAO Z.-Q., XU Z.-F., LIANG C.-S., LI L.-B., FENG J.-Y. Elemental and strontium isotopic geochemistry of the soil profiles developed on limestone and sandstone in karstic terrain on Yunnan-Guizhou Plateau, China: implications for chemical weathering and parent materials. Journal of Asian Earth Sciences, **67**, 138, **2013**.
31. ZHANG K., GAO J., MEN D., ZHAO X., WU S. Insight into the heavy metal binding properties of dissolved organic matter in mine water affected by water-rock interaction of coal seam goaf. Chemosphere, **265**, 129134, **2021**.
32. ZHAO X., XU Z., SUN Y. Mechanism of Changes in goaf water hydrogeochemistry: A case study of the menkeqing coal mine. International Journal of Environmental Research and Public Health, **20** (1), 536, **2022**.
33. FARID I., TRABELSI R., ZOUARI K., BEJI R. Geochemical and isotopic study of surface and groundwaters in Ain Bou Mourra basin, central Tunisia. Quaternary International, **303**, 210-227, **2013**.
34. MURPHY W.M., HELGESON H.C. Thermodynamic and kinetic constraints on reaction rates among minerals and aqueous solutions. III. Activated complexes and the pH-dependence of the rates of feldspar, pyroxene, wollastonite, and olivine hydrolysis. Geochimica et Cosmochimica Acta, **51** (12), 3137, **1987**.
35. SRINIVASAMOORTHY K., GOPINATH M., CHIDAMBARAM S., VASANTHAVIGAR M., SARMA V. Hydrochemical characterization and quality appraisal of groundwater from Pungar sub basin, Tamilnadu, India. Journal of King Saud University-Science, **26** (1), 37, **2014**.
36. ZHU G.F., LI Z.Z., SU Y.H., MA J.Z., ZHANG Y.Y. Hydrogeochemical and isotope evidence of groundwater evolution and recharge in Minqin Basin, Northwest China. Journal of Hydrology, **333** (2-4), 239, **2007**.
37. LASAGA A.C. Chemical kinetics of water-rock interactions. Journal of geophysical research: solid earth, **89** (B6), 4009, **1984**.
38. HUANG T.M., PANG Z.H. Changes in groundwater induced by water diversion in the Lower Tarim River, Xinjiang Uygur, NW China: Evidence from environmental

isotopes and water chemistry. Journal of Hydrology, **387** (3-4), 188, **2010**.

39. LI A.J., SCHMITZ O.J., STEPHAN S., LENZEN C., YUE P.Y.K., LI K.B., LI H.S., LEUNG K.S.Y. Photocatalytic transformation of acesulfame: Transformation products identification and embryotoxicity study. Water Research, **89**, 68, **2016**.
40. PERRY E., PAYTAN A., PEDERSEN B., VELAZQUEZ-OLIMAN G. Groundwater geochemistry of the Yucatan Peninsula, Mexico: Constraints on stratigraphy and hydrogeology. Journal of Hydrology, **367** (1-2), 27, **2009**.
41. WANG S.X. Hydrochemical and isotopic characteristics of groundwater in the Yanqi Basin of Xinjiang province, northwest China. Environmental Earth Sciences, **71** (1), 427, **2014**.
42. CRAIG H. ISOTOPIC VARIATIONS IN METEORIC WATERS. Science, **133** (346), 1702, **1961**.
43. LANDWEHR J., COPLEN T. In Line-conditioned excess: a new method for characterizing stable hydrogen and oxygen isotope ratios in hydrologic systems, International conference on isotopes in environmental studies, IAEA Vienna: 2006; 132, **2006**.
44. PANG Z.H., KONG Y.L., LI J., TIAN J. In An isotopic geoindicator in the hydrological cycle, 15th Water-Rock Interaction International Symposium (WRI), Evora, PORTUGAL, 534, **2016**.
45. HORITA J., WESOLOWSKI D.J. Liquid-vapor fractionation of oxygen and hydrogen isotopes of water from the freezing to the critical temperature. Geochimica et Cosmochimica Acta, **58** (16), 3425, **1994**.
46. GIBBS R.J. MECHANISMS CONTROLLING WORLD WATER CHEMISTRY. Science, **170** (3962), 1088, **1970**.
47. COLMAN S.M. Rock-weathering rates as functions of time. Quaternary research, **15** (3), 250, **1981**.
48. LARSON T.E., BUSWELL A.M., LUDWIG H.F., LANGELIER W. Calcium carbonate saturation index and alkalinity interpretations [with discussion]. Journal (American Water Works Association), 1667, **1942**.
49. CHARLTON S.R., PARKHURST D.L. Modules based on the geochemical model PHREEQC for use in scripting and programming languages. Computers & Geosciences, **37** (10), 1653, **2011**.
50. TENG H.H. Controls by saturation state on etch pit formation during calcite dissolution. Geochimica et Cosmochimica Acta, **68** (2), 253, **2004**.
51. FRAPE S., FRITZ P., MCNUTT R.T. Water-rock interaction and chemistry of groundwaters from the Canadian Shield. Geochimica et Cosmochimica Acta, **48** (8), 1617, **1984**.
52. CHENG Y., MAO J., YANG Z. Geology and vein tin mineralization in the Dadoushan deposit, Gejiu district, SW China. Mineralium Deposita, **47**, 701, **2012**.
53. ZAW K., PETERS S.G., CROMIE P., BURRETT C., HOU Z. Nature, diversity of deposit types and metallogenic relations of South China. Ore Geology Reviews, **31** (1-4), 3, **2007**.
54. CELEBI A., OZDEMIR S. Mining wastewater management and its effects on groundwater and ecosystems. Water Science and Technology, **70** (9), 1481, **2014**.
55. ZHANG Z., XIAO C., ADEYEYE O., YANG W., LIANG X. Source and mobilization mechanism of iron, manganese and arsenic in groundwater of Shuangliao City, Northeast China. Water, **12** (2), 534, **2020**.
56. ABBASPOUR N., HURRELL R., KELISHADI R. Review on iron and its importance for human health. Journal of research in medical sciences: the official journal of Isfahan University of Medical Sciences, **19** (2), 164, **2014**.
57. HORNING K.J., CAITO S.W., TIPPS K.G., BOWMAN A.B., ASCHNER M. Manganese is essential for neuronal health. Annual review of nutrition, **35**, 71, **2015**.